

CHARACTERIZATION OF PRE-BAKED CARBON ANODE SAMPLES USING X-RAY COMPUTED TOMOGRAPHY AND POROSITY ESTIMATION

Donald Picard^{1,2}, Houshang Alamdari^{1,2}, Donald Ziegler³, Bastien Dumas², Mario Fafard²
¹Department of Mining, Metallurgical and Materials Engineering, 1065 avenue de la Médecine
Université Laval, Québec, QC, G1V 0A6, Canada
²NSERC/Alcoa Industrial Research Chair MACE³ and Aluminium Research Centre – REGAL
Université Laval, Québec, QC, G1V 0A6, Canada
³Alcoa Canada Primary Metals, Aluminerie de Deschambault, 1 Boulevard des Sources,
Deschambault-Grondines, QC, G0A 1S0, Canada

Keywords: Carbon Anode, X-ray Computed Tomography, Density, Porosity

Abstract

Computed tomography has been used in recent years to gather information on carbon anodes which can be used to calibrate numerical models dedicated to simulate the anode forming process. To this end, samples with diameters varying from 50 mm up to 300 mm and cored from an industrial anode have been scanned in a Somatom Sensation 64. A correlation was established between the CT scan results and the apparent density. To validate the correlation, an extended campaign was performed on 50 mm diameter samples cored in 20 different anodes with the advantage of using possibly different raw materials. In addition to the CT scan results, the apparent and real densities have been experimentally measured to estimate the porosity level. Similarly to the apparent density, a correlation between the CT scans results and the porosity has been proposed.

Introduction

This paper is the sequel of the work of [1] with a focus on the carbon anode used in the aluminium industry. As already introduced in the previous work, carbon anodes are consumed during electrolysis and replaced after approximately 28 days of operation. Depending on the cell technology, approximately one anode per cell is replaced each day. Hence a large number of anodes and consequently a large quantity of raw materials are required to operate a plant. The aluminium producers deal with continuous changing of raw materials properties resulting in a wide variation of physical properties of the pre-baked anodes.

There exists a great interest to use numerical simulation methods to model the manufacturing process and to use these tools and knowledge to minimize the effect of the raw materials variation. To achieve this goal, experimental data must first be collected in order to validate the models. The first step is thus to obtain the apparent density distribution of a full-scale prebaked anode using the NDT X-Ray computerized tomography (CT) method. To do so, a CT-based method for estimation of apparent density of anode materials was developed [1] using full-scale prebaked anode core samples. This led to a linear relation between the anode apparent density and the X-ray attenuation coefficient (CT number). The relation proposed by [1] was established using core samples taken from only one anode. The next step is to validate this relation using samples from different anodes in order to include the effects of raw materials and process variations.

In the same paper, the porosity was estimated using a relation proposed for homogeneous materials [2] leading to yield overestimated values. New methods have thus been investigated

and compared to experimental measurement. It has to be noted that the goal is not to get porosity distribution; instead we planned to obtain only an average value of the porosity over the considered domain.

Methodology

X-Ray computed tomography

Core samples of 50.8 mm (2 in) in diameter were taken from industrial anodes produced at Alcoa Deschambault Smelter and scanned using a Somatom Sensation 64 at INRS-ETE research centre in Quebec City (Figure 1).

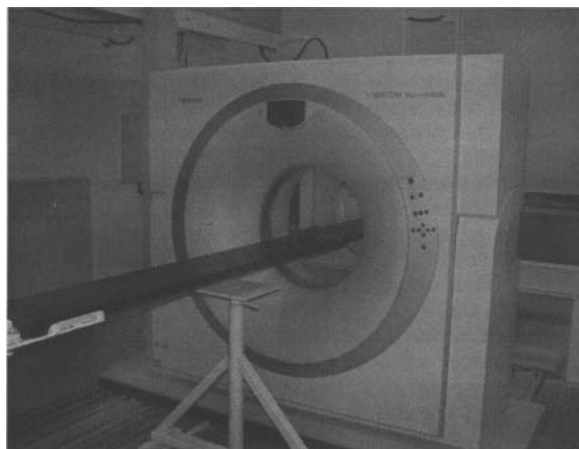


Figure 1. Somatom Sensation 64 located at the INRS-ETE (Courtesy of INRS-ETE)

In order to reveal the raw materials and process variations on the density and porosity estimation, core samples were taken from twenty pre-baked anodes (one core per anode) all at the same location within the anodes.

This method gives the so-called CT number expressed in Hounsfield Units (HU) which is related to the X-Ray attenuation coefficient [3] and generally ranges from -1000 for air to $+3000$ for very dense materials such as metals. The density of materials with low atomic number (e.g. carbon) can be estimated by assuming a linear relation between the CT number and the density [3, 4]. Previous work [1] has proposed a linear relation for pre-baked carbon anode and could be expressed as:

$$\rho = 0.0011 \times \text{CT number} + 1.1081 \quad (1)$$

Parameters of the Somatom Sensation 64 were kept the same, i.e., X-Ray tube at 120 keV and 300 mA as well as a scanning step of 0.6 mm, which also corresponds to the voxel thickness. Dimensions of the acquired image were $60 \times 60 \text{ mm}^2$ with a pixel resolution of 512×512 . Hence, the voxel size of a sample of 50.8 mm diameter is $0.1171875 \times 0.1171875 \times 0.6 \text{ mm}^3$.

Apparent and real density measurement

Following the CT scan, anode core samples were cut in slices of 15 mm thick on which apparent density and real density were experimentally measured. Each slice is numbered as shown in Figure 2. The number of slices per core varies (between 14 and 17) as a function of the length of each core.



Figure 2. Slice numbering of core sample

The slice thickness was chosen based on the volume capacity of the gas pycnometer used for the real density measurement. The porosity was then calculated based on the apparent and real densities.

The apparent density was calculated with two different methods. The first one refers to the ISO 12985-1:2000(E) standard method; the samples were weighed with a precision balance (Sartorius CPA16001S) and dimensions were measured using a pair of calipers (Mitutoyo CD-12" PSX). The apparent density measurement using this method is termed "Geometry". The second method is based on the water displacement principle to determine sample volume. The apparatus used is shown in Figure 3. Water is poured in a machined steel tube container and water height variation caused by the sample immersion is measured using a plastic float attached to a high precision linear displacement device (Heidenhain® MT 1281). Anode samples were previously coated with a known volume of paraffin to prevent water penetration. This method will later be termed as "Water" in this paper. However, this method led to some repeatability problems of the measurement mainly caused by surface oscillation occurring during the insertion of the sample in the water container and thus inducing a bias error in the measured displacement value of the float. Comparison between these two methods is discussed in the next section.



Figure 3. Water displacement apparatus

Real density was thereafter measured using pycnometry. A slice sample was first crushed down to few micrometers and weighed on the precision balance. The resulting powder volume was then measured using a helium pycnometer (AccuPyc II 1340).

Porosity of slices, with either the Geometry or Water method, was then calculated using the following relation:

$$\text{Porosity} = 1 - \frac{\text{Apparent density}}{\text{Real density}} \quad (2)$$

Estimation of porosity level using CT scan

As mentioned earlier, the porosity level estimation had to be reviewed. Four methods have been tested to estimate this parameter. The first is the one that has already been reported by [1]. It is called "CT max 980" based on the fact that the maximum CT number allowed (CT_{\max}) is 980 HU. The porosity is estimated using the following relation:

$$\text{porosity}|_{CT_{\max 980}} = \left(1 - \frac{\overline{CT} + 1024}{CT_{\max} + 1024} \right) \quad (3)$$

where \overline{CT} is the average CT number of the volume considered. The second method was proposed by [5] for hydrocarbons and is derived from Digital Terrain Model (DTM). To facilitate the computation, an offset of +1000 was applied to the data set in order to get only positive values, i.e., $0 < CT_{\text{number}} < CT_{\max} + 1000$. The porosity is then estimated using the following equation:

$$\text{porosity}|_{\text{Taud et al.}} = \min \left(\phi(l) = \frac{\sum_{i=0}^l (l - r_i) H(r_i)}{l \sum_{i=0}^l H(r_i)} \right) \quad (4)$$

where r_i is a grey level related to the altitude, $H(r_i) = n_i/n$, n_i is the number of voxel in the sample slice with grey level r_i , n is

the total number of voxel in the sample slice and l varies from 0 to CT_{max} .

The third method used for porosity estimation consists of determining a threshold value below which voxels are considered as void. Contrary to the “classical” threshold methods as discussed by [5], the method presented here is not meant to distinguish void from solid. In fact, most of the porosity in the anode material is smaller than the voxel size. Porosity is thus observed mainly through density variation (grey level variation). A threshold value is found for each slice through an iteration process based on the apparent density measured with the water displacement method. The choice of the “Water” apparent density will be explained in the next section.

The last method simply calculates the porosity with Eq. (2) using an average value of real density and an apparent density obtained by calculation using Eq. (1).

One core sample was used to test and calibrate the apparatus, and the data obtained with this sample are considered irrelevant. Therefore, the results are reported for 19 samples instead of 20.

Results and discussion

X-ray computerized tomography

X-ray computerized tomography was performed on all core samples. Typical CT scan images are shown in Figure 4 and Figure 5.

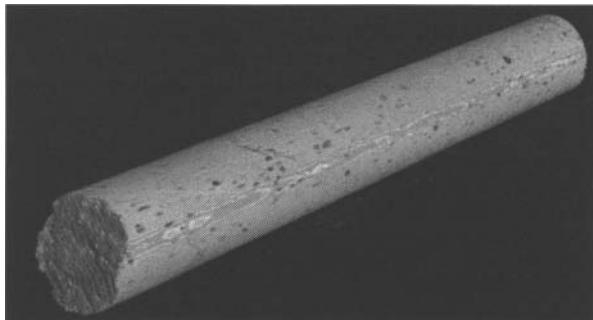


Figure 4. 3D view of typical CT scan on a 50.8 mm anode core

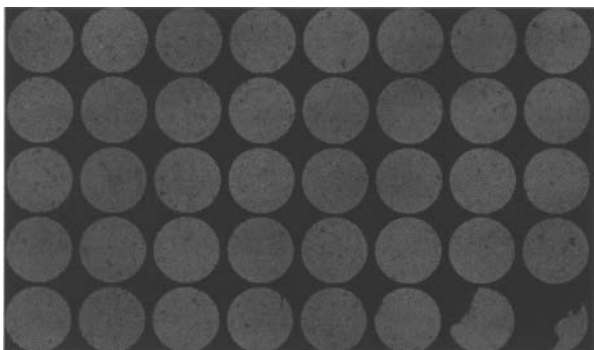


Figure 5. Cross-sectional views of typical CT scan on a 50.8 mm anode core

As observed previously [1], aggregates and large porosity (dark zones) as well as dense impurities (white spots) are clearly visible. Even at a very small volume fraction, those impurities caused an overestimation of the porosity when using Eq. (3) thus, having a limit for the maximum value of CT_{max} was necessary. A typical voxel distribution of a core slice is shown in Figure 6. This distribution highlights the fact, based on the negative skewness of that distribution, that there are two distinguishable phases (large pores and carbon based materials) within the analysed volume and for a given voxel resolution. Considering that the theoretical CT number of graphite is 980 HU and the fact that the average value of a typical voxel distribution is close to 500 HU, it can be assumed that the size of most of the porosity is lower than the voxel resolution, i.e., most of the voxel represents an average value of a carbon/air mixture.

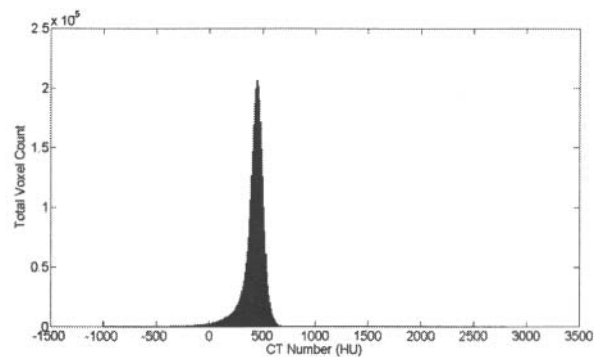


Figure 6. Typical voxel distribution of a core slice

Increasing the core sample diameter will further increase the voxel volume and will result in voxel distribution more uniformly distributed or in a skewness of the distribution near zero.

Apparent and real densities

As mentioned earlier, the apparent density was measured using two different methods: Geometry and Water. Figure 7 shows the average value of the apparent and real densities measurements for all core samples as a function of the slice position and Table I shows their standard deviations. The number of values used to calculate the average and standard deviation values varies from slice number 14 to 17 due to length variation of the samples.

The first observation to be noted is the high standard deviation of the apparent density measured with the water displacement method (Water) compared to the geometrical one (Geometry). In fact, the standard deviation obtained with the Water method is almost twice of that obtained with Geometry one. This observation is a direct consequence of the repeatability problem described earlier in the Methodology section.

Figure 7 also shows the apparent density estimation obtained from the CT scan results and using Eq. (1). Comparison with the measured apparent densities was performed by calculating the error between the average CT scan estimations and measured values. The result is shown in Figure 8 and clearly indicates that CT scan results correlate better with the apparent density measured by water displacement. Therefore, despite the high standard deviation values, subsequent results will be compared or

derived from apparent density obtained with the water displacement method.

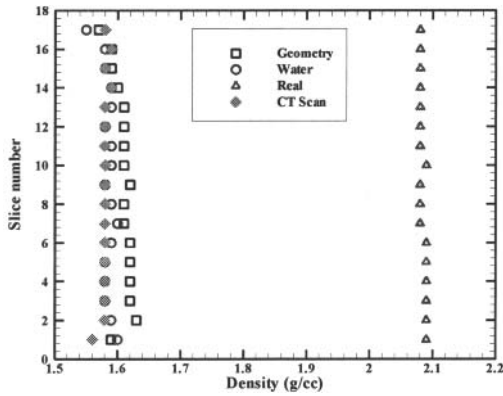


Figure 7. Average apparent (\square , \circ , \diamond) and real densities (Δ) of core samples as a function of the slice position

Table I. Standard deviation of the average apparent and real densities (g/cc) as a function of the slice position

Slice number	Geometry	Water	CT Scan	Real
17	0.03	0.03	0.02	0.01
16	0.02	0.02	0.01	0.01
15	0.02	0.03	0.01	0.01
14	0.02	0.04	0.01	0.01
13	0.03	0.08	0.01	0.02
12	0.02	0.04	0.01	0.01
11	0.03	0.06	0.01	0.01
10	0.03	0.04	0.01	0.01
9	0.03	0.07	0.01	0.01
8	0.03	0.06	0.01	0.01
7	0.03	0.07	0.01	0.01
6	0.03	0.07	0.01	0.01
5	0.03	0.07	0.01	0.02
4	0.02	0.05	0.01	0.01
3	0.03	0.06	0.01	0.01
2	0.02	0.06	0.02	0.01
1	0.02	0.06	0.02	0.01

Figure 8 also shows a tendency for slices 13 to 17 on the geometrical apparent density. There is however no clear explanation for it.

The second observation to be noted is the variation of the real density as a function of the slice position. The real density remains almost constant with slice position compared to the apparent density. This observation outlines the fact that, in the present study, the apparent density variation comes from porosity variation rather than material density variation (coke/pitch/butts).

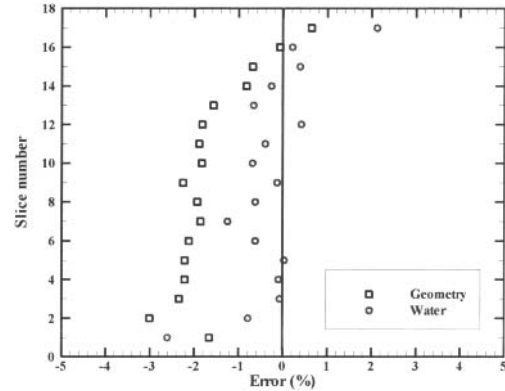


Figure 8. Error distribution on the estimated apparent density- \square CT scan vs Geometry, \circ CT scan vs Water

Porosity estimation

Four methods were used to estimate the porosity level of the samples. Figure 9 shows the results obtained with three of those methods (CT max 980, Threshold and Eq. (2)), compared with the experimental ones. In the case of the Threshold method, a mean threshold value was previously estimated by averaging all values obtained on all core slice samples. The threshold value obtained, based on the “Water” apparent density for the reason aforementioned, is 400 HU. Estimation of the porosity with the use of Eq. (2) also required the determination of the real density. It was however shown earlier that, for the present work, the real density can be considered constant having a known value.

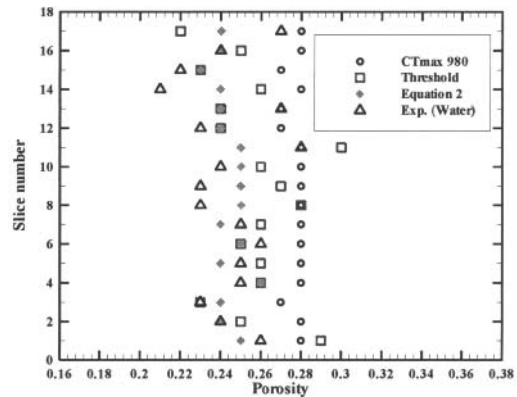


Figure 9. Porosity level estimation of a representative sample

The first observation on the porosity level results is the constant overestimation of porosity while using the CTmax 980 method. However, results obtained with the two other methods seem to be comparable. As with the apparent density, the estimation error of each method was compared to the experimental results and is shown in Figure 10.

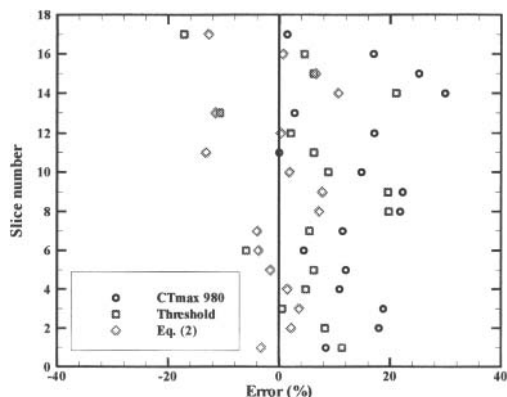


Figure 10. Error distribution on porosity level estimation

Figure 10 shows that the error of porosity level estimation is high compared to that of the apparent density ones. In fact, errors range between -10% and +10% for the threshold and Eq. (2) methods. Still, the best estimation tends to be obtained using the simplest method; i.e., Eq. (2). The threshold method gave also good result but problems may occur if there are high apparent density gradients within the sample. Figure 11 shows the evolution of threshold values as a function of the measured apparent density with the water displacement method. 17 values comprising of each threshold value and the apparent density were averaged for each slice position..

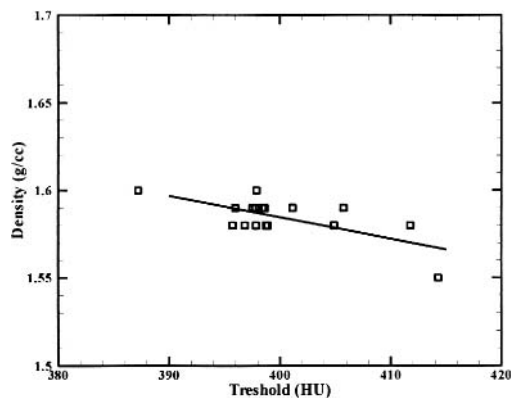


Figure 11. Threshold evolution as a function of the apparent density (Water)

Therefore, estimation error will vary as a function of the apparent density. This is however not surprising since the determination of the threshold was first based on the apparent density value. Another assumption was that threshold value could also vary with porosity distribution. In fact, increasing pore size (or decreasing voxel volume) should also decrease the skewness (increase in absolute value) of the voxel distribution (ref. to Figure 6 and the related explanation). Figure 12 shows the skewness of the voxel distribution for each slice of a representative sample. There is no clear tendency found in Figure 12 and thus it can be assumed that the threshold evolution observed in Figure 11 comes from the

increase of porosities that were smaller than the CT scan resolution (or voxel volume).

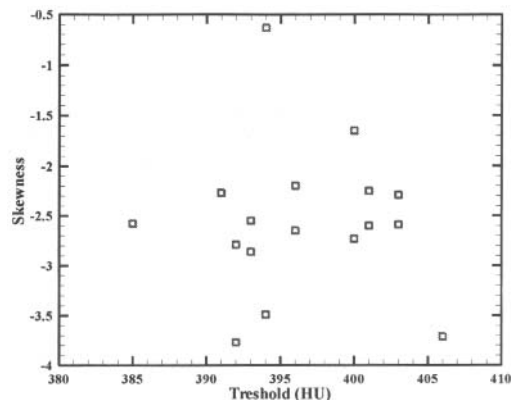


Figure 12. Skewness of the voxel distribution as a function of the threshold value

The last method used to estimate the porosity was based on the work of [5]. A computation of the method was performed on the representative sample and the results are shown in Figure 13. Porosity level corresponds to the minimum value of the function. Based on these results, the porosity level is close to 0.15 with a threshold value near 550 HU (after subtracting the offset value of +1000). These values are not close to those obtained above with the other methods. In addition, the porosity level estimated with this method is also too low. This method was not investigated further.

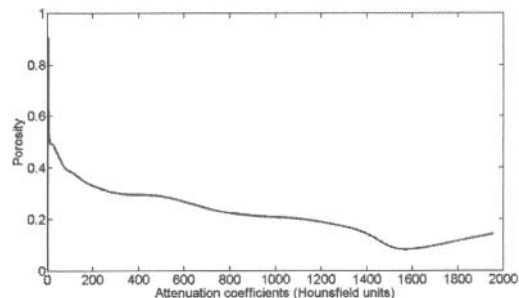


Figure 13. Porosity estimated based on DTM [5]

Conclusion

Pre-baked anode core samples were used in a previous work to propose a linear relation between the pre-baked anode apparent density and the X-ray attenuation coefficient. The present work analyzed nineteen pre-baked anode cores to validate the proposed linear relation. Validation was based on apparent density measurement with two different methods; i.e., with geometrical estimation of the volume of sample slice and with water displacement. It must be noted that there are advantages and disadvantages associated with both methods. Apparent density estimated by CT scan correlated better with the apparent density measured experimentally using the water displacement method ($\pm 1\%$). This latter method also allows geometrical irregularities to be taken into account easily.

The porosity level was estimated using four methods, including the one introduced in the previous work. Porosity level estimation based on the DTM method didn't give relevant results; on the other hand, the CT max 980 still overestimated the porosity level. Better results were obtained with the other two methods ($\pm 10\%$). Nevertheless, the threshold method seems to be more sensitive to apparent density variations. Assuming that the real density of the given pre-baked anodes is known, the method based on Eq. (2) is reasonably considered as the one to be used for estimation of the porosity level with the CT scan results for the purpose of this work.

Acknowledgements

The authors gratefully acknowledge the financial support provided by Alcoa Inc., by the Natural Sciences and Engineering Research Council of Canada and the technical support of the Aluminium Research Centre – REGAL. The authors would also like to thank Amélie Dufour for her help.

References

1. Picard, D., et al., *Characterization of a full-scale prebaked carbon anode using X-ray computerized tomography*. Light Metals 2011, 2011: p. 973-978.
2. Boespflug, X., et al., *Axial Tomodensitometry - Relation between the CT Intensity and the Density of the Sample*. Canadian Journal of Earth Sciences, 1994. **31**(2): p. 426-434.
3. Adams, A.N., et al., *The non-destructive 3-D characterization of pre-baked carbon anodes using X-ray computerized tomography*. Light Metals, 2002: p. 535-539.
4. Duchesne, M.J., et al., *A rapid method for converting medical Computed Tomography scanner topogram attenuation scale to Hounsfield Unit scale and to obtain relative density values*. Engineering Geology, 2009. **103**(3-4): p. 100-105.
5. Taud, H., et al., *Porosity estimation method by X-ray computed tomography*. Journal of Petroleum Science and Engineering, 2005. **47**(3-4): p. 209-217.